Available online at www.sciencedirect.com
SCIENCE DIRECT®
Polymer 45 (2004) 1223–1234
polymer
www.elsevier.com/locate/polymer

Flow-induced chain scission as a physical route to narrowly distributed, high molar mass polymers

Brett A. Buchholz[a], Jacob M. Zahn[a,1], Martin Kenward[b], Gary W. Slater[b], Annelise E. Barron[a,*]

[a]*Department of Chemical Engineering, Northwestern University, 2145 Sheridan Road, Room E136, Evanston, IL 60208, USA*
[b]*Department of Physics, University of Ottawa, 150 Louis-Pasteur, Ottawa, Ont., Canada K1N 6N5*

Received 18 August 2003; received in revised form 12 November 2003; accepted 17 November 2003

Abstract

We present data showing a substantial narrowing of the polydispersity index (PDI) of high polymers occurring as a consequence of random chain scission events in a transient elongational flow field. In our experiments, semi-dilute aqueous solutions of high-molar mass, polydisperse polymers (PDI > 1.4) were injected under pressure through an elongational flow field at the entrance of a capillary tube (i.d. 250 μm). Chain scission events occurring during multiple passes through the capillary entrance cause a marked decrease in PDI, to values as low as 1.12, along with the expected decrease of the average molar mass. The phenomenon appears to be entirely physical and independent of the chemical nature of the polymer, since similar results are obtained with polyacrylamide, polydimethylacrylamide, and poly(ethylene oxide). Statistical modeling of the evolution of the polymer molar mass distribution shows the results to be consistent with the random scission, near the mid-point, of those polymer chains that exceed a certain flow field-dependent critical chain length.

Keywords: Polymer degradation; Scission; Extensional flow

1. Introduction

Monodisperse high molar mass polymers are of interest for a number of industrial and research applications requiring stringent levels of material characterization and specific polymer phase behaviors [1–4]. A few chemical methods currently exist that allow the generation of low-polydispersity index (low-PDI) polymers with high molar mass. For example, in living polymerization, chain propagation proceeds, ideally, without termination or chain transfer [5]. If short chains are terminated early, they may be 'revived' in some approaches by the use of highly active metallic catalysts and carried out to a target molar mass, producing a relatively narrow molar mass distribution even for large polymers. However, because of side reactions that can occur in some cases, living polymerization gives access to low-PDI high polymers (i.e. polymers with PDI < 1.20 and $M_w > 200,000$ g/mol) of many, but not all chemical classes [5,6]. One important living polymerization method for the preparation of monodisperse polymers is ring-opening metathesis polymerization (ROMP), which involves the catalytic polymerization of strained cyclic olefins in a variant of the olefin metathesis reaction [3,5,7–9]. The high activity of catalysts used in ROMP can cause intermolecular reactions in some classes of monomers, which can broaden the final molar mass distribution [5]. Generally, living polymerization methods require carefully controlled reaction conditions and special metallic catalysts [10], and are most convenient to use for those polymeric species without reactive side-chains and subgroups, unless protecting groups are employed. In the following, we present an entirely different route to the generation of low-polydispersity polymeric materials of high molar mass, by a physical method that exploits an iterative process of controlled polymer degradation in a transient extensional flow field. Before describing the method and our results, we give background on prior, related observations.

It has long been known that high shear from mechanical action can cause chemical bonds in polymer chains to break [11]. Some of the earliest work in this area used statistical methods to treat a process of random chain scission

* Corresponding author. Tel.: +1-847-491-2778; fax: +1-847-491-3728.
E-mail address: a-barron@northwestern.edu (A.E. Barron).
[1] Present Address: Department of Chemical Engineering, Stanford University, Palo Alto, CA 94305, USA.

0032-3861/$ - see front matter © 2003 Elsevier Ltd. All rights reserved.
doi:10.1016/j.polymer.2003.11.051

[12–14]. Most of these early theoretical studies modeled initial polymer populations that were monodisperse (PDI = 1.0). Since then, the mechanical degradation of polymers in elongational flow fields, which leads to a reduction in average polymer molar mass, has been widely observed and studied. Passage through an elongational flow field exerts strong hydrodynamic forces upon a coiled polymer molecule in solution, causing it to stretch, orient and extend in the direction of flow. If elongational forces on the molecule are sufficiently strong, and the rate of chain stretching far exceeds the rate of chain relaxation, the polymer backbone can be severed. The precise mechanism of chain scission is not fully understood, and remains a matter of discussion in literature [15–20]. It was theorized in 1944 by Frenkel that as the molecule becomes elongated in the direction of flow, the forces acting upon the molecule are greatest at its center [15], which can lead in turn to chain scission near the middle of the chain.

Several different flow geometries can lead to the creation of an elongational flow field. Generally, sudden contractions in the direction of flow generate a transient elongational effect, as velocity streamlines converge, which is localized in the region of the contraction. Full elongation of polymer chains most likely only occurs along the centerline of the flow field, where the molecules should not experience any shearing deformations [21]. Merrill and Leopairat designed an apparatus with a contraction ratio of 37.5 and demonstrated that chain scission occurred near the center of the molecule. They also were able to show that with an increase in the number of passes through the orifice, the net number of molecules that had experienced scission increased [22]. Nguyen and Kausch have performed extensive studies of polymer degradation in convergent flow using contraction ratios similar to those of Merrill and Leopairat [19,23–26]. Along with the expected reduction in molar mass, these authors observed a slight narrowing of the PDI of a high molar mass polystyrene sample as the total number of midpoint scission events increased [23]. At an applied strain rate of 275,000 s^{-1}, a significant fraction of the polymers were found to undergo two degradation events during a single pass through the contraction [26]. In these transient elongational flow fields, polymer degradation was found to occur even when the residence time was insufficient to allow full elongation of the polymer molecules, and thus midpoint scission occurred in partially uncoiled polymer molecules. Other researchers have also studied the flow of polymer solutions through transient extensional flow fields created by an abrupt contraction, using contraction ratios on the order of 4:1 or 8:1 [27–30].

So-called constant or homogeneous elongational flow fields, which can also lead to flow-induced chain degradation, are more difficult to achieve physically. The use of a cross-slot device, which generates an opposing-jets geometry, can create an elongational effect in which a given fluid element or polymer molecule will have a residence time long enough to achieve a constant strain rate. The geometry generates a stagnation point (zero velocity point) in the center of the flow field, where the molecules can experience full elongation. Hence, in a cross-slot device, chain extension is limited to a small area of the flow field. These quasi-steady-state flow fields have been studied by Odell and Keller and colleagues [20,31–38]. Owing to the small number of molecules that pass close to the stagnation point and undergo elongation and chain scission, a large number of passes through the system, at least 250, typically are needed to observe central chain scission [35]. Birefringence measurements were used to determine the extent of chain elongation [35]. In both transient and constant elongational flow fields, the critical fracture strain rates for chain scission are observed to decrease with increasing molar mass, with the specific dependence on molar mass (M^{-1} or M^{-2}) differing as a function of the instrument and conditions used [24,37].

In at least two other degradation studies in addition to that of Nguyen and Kausch mentioned above [23], a decrease in the polydispersity of a polymer solution was observed under some conditions [39,40]. For example Ballauff and Wolf [39] examined the shearing of polystyrene in *trans*-decalin using a Couette device, while Tanigawa et al. [40] studied the degradation by ultrasonication of three nucleic acid polymers in water. For one of the DNA solutions, a reduction in PDI from 1.7 to 1.2 was reported (for DNA polymers with initial M_w of 3.1×10^5 g/mol and final M_w of 6.4×10^4 g/mol). However, such significant PDI reductions have not been shown for any other polymer classes, nor achieved by any other degradation method besides sonication.

In this work, we examine the evolution of the molecular mass distribution of three different, initially very polydisperse and high-M_w ($> 2.5 \times 10^6$ g/mol) polymer solutions as they are forced through a sudden constriction (contraction ratio ~ 100:1) comprising a 250 μm-ID capillary. To our knowledge, this is the first polymer degradation study involving iterative capillary entrance flow; we have examined the effects of this treatment on three industrially important water-soluble polymers, including linear polyacrylamide (LPA), polydimethylacrylamide (pDMA), which should have backbone–backbone bonds of similar intrinsic strength, and poly(ethylene oxide) (PEO). Our experimental results show that with multiple passes through the constriction, the expected progressive reduction in weight-average molar mass (M_w) is accompanied by a remarkable drop of the PDI for all three polymer samples, to values in the range of 1.12–1.15.

In order to better characterize this process, we also developed and applied to the data a simple statistical model with three physically motivated free parameters. One goal of this modeling study was to show that, based on a few reasonable assumptions having a firm basis in the literature, we could explain the dramatic PDI reductions that we observe. Analysis of the experimental data with this model indicates that the evolution of the molar mass distribution

can be explained by a sequence of chain scission events, where the probability of breakage increases sharply beyond a flow field-dependent critical molecular size. We also conclude based on this analysis that scission occurs predominantly in the central $\cong 20\%$ of the chain.

2. Experimental

High molar mass, polydisperse polymers ($M_w > 2.5 \times 10^6$ g/mol, PDI > 1.4) were injected in aqueous solution into fused-silica capillaries (Polymicro Technologies, Phoenix, AZ) by means of a custom-built pressure-loading device (Fig. 1). LPA (M_w 4.10×10^6 g/mol) and pDMA (M_w 4.30×10^6 g/mol) were prepared by free-radical polymerization. Acrylamide (Amresco, Solon, OH) and *N*,*N*-dimethylacrylamide (Monomer–Polymer and Dajac Labs, Inc., Feasterville, PA) were polymerized in an aqueous solution (7.0% (w/v) total monomer concentration, thermostated at 47 °C and degassed with nitrogen prior to initiation). Initiator V-50 (2,2′-azobis(2-amidinopropane) dihydrochloride, Wako Chemical USA, Inc., Richmond, VA) was dissolved in water and injected into the reaction flask. After the reaction was complete, the resulting solution was dialyzed for 10 days against distilled water and then lyophilized to recover the dry polymer. PEO (M_w 2.68×10^6 g/mol) was obtained from Aldrich Chemical Company (Milwaukee, WI).

The polymer samples were dissolved at low, dilute to semi-dilute concentrations (0.1% (w/v) and 0.3% (w/v)) in water. At such low concentrations, the viscosities of the solutions are not much higher than that of water

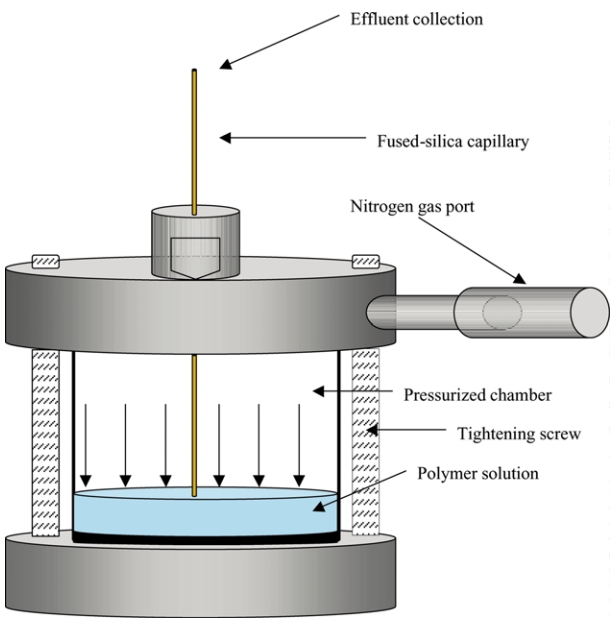

Fig. 1. A schematic illustration of the custom-built, aluminum pressure-loading device with a suspended capillary.

(< 5 cP). At such low viscosities, the effects of shear thinning of the polymer solutions is expected to be minimal. The pressure-loading device (shown in Fig. 1) holds a charge of approximately 9 ml of polymer solution and was manufactured at Northwestern University. The top, bottom, and main body of the pressurized chamber are made out of aluminum. In addition to three screws that are used to tighten the device, O-rings on both the top and bottom of the pressurized chamber aid in sealing it. The capillary is extended into the polymer reservoir from the top of the device and sealed with a Swagelok™ valve. A side-mounted gas port allows the application of nitrogen gas in the pressurized chamber to propel the polymer solution from the reservoir through the capillary. In different experiments, the injection pressure was varied from 500 to 1000 psi (3.5–6.9 MPa); each run was performed at constant applied pressure. Capillaries used for different experiments had various inner diameters, ranging from 75 to 324 μm, and were cut to a length of 10–20 cm with a diamond capillary cutter to ensure a flat orifice, as confirmed after cutting by optical microscopy.

Injected polymer was collected in a reservoir and re-injected 4 additional times, for a total of 5 passes through the contraction defined by the capillary entrance. After each pass through the capillary entrance, a portion of the sample solution (~ 1 ml) was collected and lyophilized, and then analyzed by gel permeation chromatography (GPC) (Waters 2690 Alliance Separations Module, Milford, MA, with Shodex (New York, NY) OH-pak columns SB-806 HQ, SB-804 HQ, and SB-802.5 HQ connected in series) in tandem with a multi-angle laser light scattering system (MALLS) (DAWN DSP Laser Photometer and Optilab DSP Interferometric Refractometer connected in series (both from Wyatt Technology, Santa Barbara, CA)), in order to determine the molar mass distribution, the weight-average molar mass, and the PDI of the polymers [41]. The columns were kept at 25 °C and the aqueous mobile phase used contained 0.1 mNaCl, 50 mM NaH_2PO_4, and 200 ppm NaN_3 (pH 4.6). To ensure that there was always enough sample for analysis after the fifth pass through the capillary, in some cases we did not collect a polymer sample after the third pass. During polymer analysis, the flow rate through the GPC columns was kept extremely low (0.3 ml/min) in order to eliminate any possibility of additional degradation of the polymer molecules during passage through the columns. We confirmed that no polymer degradation occurred at this flow rate in a separate study (data not shown).

Capillary viscometry was performed to determine the characteristic relaxation time of the polyacrylamide sample used in one set of experiments. Solution concentrations of 0.20–1.99 mg/ml were analyzed using an Ubbelohde capillary viscometer. A plot of reduced viscosity vs. concentration was used to determine the intrinsic viscosity ($[\eta]_o$). The characteristic relaxation time τ_o was estimated

with the equation [42]:

$$\tau_o = \frac{[\eta]_o M_w \eta_s}{N_A k_B T} \quad (1)$$

where η_s is the viscosity of the solvent, N_A is Avogadro's number, k_B is Boltzmann's constant, and T is temperature.

A schematic diagram of the converging streamlines in the elongational flow field created by the device, and their likely effect on polymer conformation for the majority of the experiments, is shown in Fig. 2. Individual polymer chains in a solution have a random coil conformation when unperturbed. As the polymer chains begin to enter the flow field they start to uncoil and stretch. Based on the observations of others [19,23–26], it is likely that some, but not all, chains become fully elongated as schematically shown in the diagram. Regardless of what fraction of chains are fully extended, it has been shown that chains only partially uncoiled can also break [26]. Given the simple design of the device and the goals of our experimental study, we did not attempt to determine to what extent polymers were stretched in the transient flow field we created. Instead, the experiments examined the effects of capillary entrance flow on the molar mass distributions of three distinct, high-M_w polymer samples in aqueous solution.

3. Results and discussion

3.1. Experimental results

Results of the experiments are shown in Fig. 3(a)–(c), in

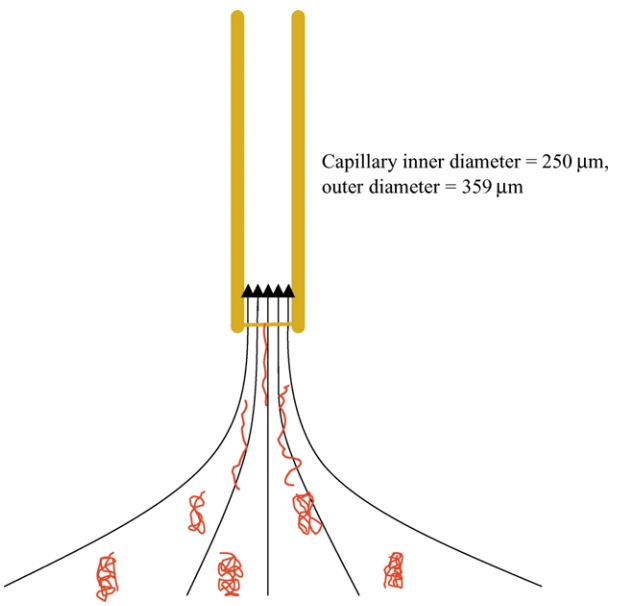

Fig. 2. Schematic illustration of the elongational flow field created by the pressure-loading device at the capillary entrance. Individual polymer chains in a dilute solution have a random coiled conformation when unperturbed. As the polymer chains begin to enter the flow field they start to uncoil and stretch, and in some cases can become fully elongated as schematically shown in the diagram.

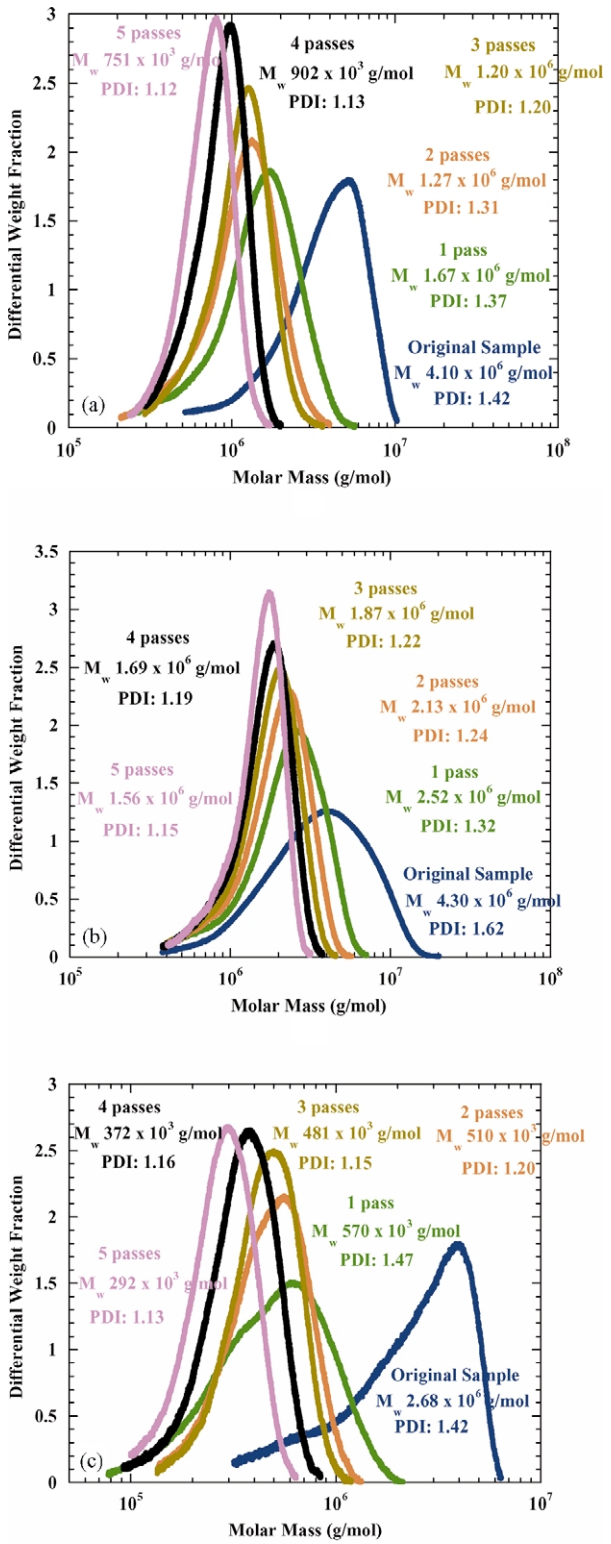

Fig. 3. Tandem GPC-MALLS characterization results obtained for (a) linear polyacrylamide, (b) polydimethylacrylamide, and (c) poly(ethylene oxide) in aqueous solution. The applied pressure was 1000 psi with a polymer solution concentration of $c = 0.1\%$ (w/v) in a 15 cm long capillary with an inner diameter of 250 μm.

plots of differential weight fraction vs. polymer molar mass. Each experiment for which results are shown in these figures was performed with a polymer solution concentration of $c = 0.1\%$ (w/v) using a 15 cm long capillary with an inner diameter of 250 μm, and an applied injection pressure of 1000 psi. In these figures, the integrated area under a given peak represents the normalized sum of the total polymer mass in the sample. As expected from previous work in the field, the average polymer molar mass decreases progressively after each pass through the capillary entrance (the peaks move to the left). However, of chief interest is the observation that the PDI of the degraded polymer samples also decreases sharply, even after only one injection through the capillary entrance. As can be seen in these plots, similar results were obtained for LPA (Fig. 3(a)), pDMA (Fig. 3(b)), and PEO (Fig. 3(c)), and the progressive effects of capillary entrance flow are particularly clear for the pDMA sample. With the decrease of the PDI, the molar mass distribution peaks increase in height after each subsequent pass, as expected.

Two aspects of the results shown in Fig. 3(a)–(c) should be stressed here. First, the molar mass distribution function changes most dramatically during the first pass. This seems to indicate, as would be expected, that it is easier to break longer molecules in a fixed elongational flow field. Second, the peaks apparently converge towards an asymptotic molar mass distribution for a large number of passes, a demonstration that, as expected from previously published studies, there is minimum (critical) molecular size below which the fixed flow field we generated is unlikely to lead to further chain scission events [43–46]. Both the average molar mass and the PDI continue to decrease after the first few passes, but at a much reduced pace. What is novel about these findings is our discovery that iterating the scission process quickly decreases not only the average molar mass but also the PDI, the latter to values of 1.15 or less in all three cases. To our knowledge, linear polyacrylamide, which has chemically labile side-chains, cannot be synthesized to such high molar mass ($M_w = 0.751 \times 10^6$ g/mol) with a PDI as low as this (1.12, the result obtained after five passes in Fig. 3(a)) by chemical methods, including living polymerization. We also note that to obtain a pDMA sample of such high average molar mass (1.56×10^6 g/mol) and low PDI (1.15), as shown in Fig. 3(b) (the fifth pass curve) would also most likely be difficult or impossible by chemical approaches.

Using the simple equation [47]

$$c^* = \frac{M_w}{\frac{4}{3}\pi N_A R_g^3} \tag{2}$$

where N_A is Avogadro's constant and R_g is the weight-average radius of gyration of the polymer obtained from the light scattering measurements, we estimated the entanglement threshold concentration, c^*, for each polymer sample studied. It has been shown that polymer coil overlap can be a factor in the degradation process and that entangled polymers experience greater tension near their midpoint than isolated polymer chains [44,46]. An increase in polymer concentration past the point of entanglement has also been determined to cause a corresponding increase in flow-induced chain scission [39]. We estimated using Eq. (2) that the initial (zero-pass) polymer solutions were slightly above their entanglement thresholds for LPA and pDMA ($c/c^* \sim 1.5–2.0$), and below c^* for consecutive passes. The PEO solution was near or above its entanglement threshold for all passes ($c/c^* \sim 1.5 - 3.0$). Hence there could be some effect of polymer–polymer entanglements on the chain scission process during capillary entrance flow, but the impact of this is most likely not dramatic since similar results were obtained in all cases.

In experiments such as these, determination of the amount of strain imparted on the viscoelastic fluid is important because, when coupled with information about the average polymer relaxation rate, one can predict the likely effect on polymer conformation. In dimensionless form, this is described by the Deborah number (De), which is the ratio of the characteristic relaxation time of the polymer solution to the characteristic flow time of the system [48]. If De is large, polymer molecules that become elongated in the flow field will not have time to relax their conformations during their residence in the elongational flow field. Capillary entrance flow is complex; fluid elements experience rapid elongation, but their elongation rate is inhomogeneous in both time and space. Using the method of Metzner and Metzner [21], we estimated the characteristic elongational strain rate under our experimental conditions to be about 45,000 s^{-1}. Viscometry data and Eq. (1) were used to determine the characteristic relaxation time for the zero-pass polyacrylamide solution to be approximately 2.6 ms. Correspondingly, the Deborah number was found to be on the order of 550. Due to the uncertainty in our estimate of the elongational strain rate, this De is only an approximation; however, clearly polymers are being stretched in the transient elongational flow field much more rapidly than they can relax.

Additional, exploratory experiments under a variety of conditions were performed using LPA solutions (data not shown), and these studies are still ongoing and will be discussed in detail in a future publication. In particular, we have investigated the impact of varying the initial polymer concentration, capillary inner diameter, and injection pressure over a limited range. We found that varying the applied pressure from 500 to 1000 psi (3.5–6.9 MPa) affected the final average molar mass, but did not significantly change the final PDI obtained. Specifically, at an injection pressure of 1000 psi, after five passes through the 250 μm capillary, a final M_w of 0.751×10^6 g/mol was obtained. Reducing the injection pressure to 750 and 500 psi led to successively higher final M_w values (1.2×10^6 g/mol and 1.4×10^6 g/mol, respectively). Hence, as would be expected, the polymer breakage process is significantly

affected by the applied strain rate: as the injection pressure is decreased, the strain rate is decreased. Therefore, the M_w after a fixed number of passes is larger for lower applied strain rates, as the size of the smallest molecules that undergo degradation is then also larger. Here a two-fold decrease of the pressure led to an approximately two-fold increase of the average molar mass, indicating that the critical molecular size is roughly inversely proportional to the strain rate. Interestingly, all three experiments produced virtually identical final PDI values, approximately 1.12, indicating that there was still a systematic reduction of the PDI with each pass and that the fundamental mechanistic process at the capillary entrance was not changed much by this two-fold reduction in applied pressure. The applied pressure thus appears to be a critical parameter for the control of the final average molar mass of the polymers, but has much less impact on PDI.

When we increased the LPA solution concentration from 0.1% (w/v) to 0.3% (w/v), we obtained results that were similar to those shown in Fig. 3(a), but which were less dramatic with respect to both the extent of chain breakage and the narrowing of PDI. Once again, the majority of breakage of LPA polymer chains occurred on the first pass through the system. After the fifth pass, the corresponding M_w was approximately 60% higher than the results obtained for 0.1% (w/v). This demonstrates that with even a slight increase of polymer concentration ($c/c^* \sim 6.0$ for the original 0.3% solution), the strain rate and elongational forces experienced by the polymers is affected. After five passes for this solution, c/c^* was reduced to about 1.2.

Although shear forces and turbulent extensional forces in tube flow are also known to have degradational effects on polymers [49], changing the length of the capillary tube from 15 to 10 or 20 cm resulted in no significant change in either final molar mass or final polydispersity. (Note that 10 cm was the shortest length that could be practically implemented with the flow device) That is, a shorter or longer exposure to the flow field in the capillary lumen did not affect the extent of chain scission that occurred. This is interesting because for all of the experiments for which results are shown in Fig. 3(a)–(c), we estimated that the Reynolds number of flow within the capillary tube exceeded the turbulent boundary ($Re > 2200$); a value of ~ 6600 was typical for experiments with the 250 μm-i.d. tube and 1000 psi applied pressure. In any case these results indicate that elongational deformations of polymer conformation at the capillary entrance are the dominant factor in polymer degradation. This has also been found in previous studies of contractile flows [50].

While results were on the whole very reproducible, our control over this chain scission process to produce polymers with a tailored, final average molar mass is relatively coarse with this apparatus. Further study, including the effect of temperature, will show whether this procedure can be tuned to generate monodisperse polymers of particular, designed molar mass.

3.2. Statistical model

In order to better understand our results and gain insight into the physical mechanisms that lead to this dramatic narrowing of PDI, we have developed a simple statistical model which captures the essential properties of the chain breakage process. We hoped to show that, using a model based on a few reasonable assumptions having a firm basis in the literature, we could explain the dramatic PDI reductions we observe. Our model is a variant of the form used by Ballauf and Wolf [16,39], Tanigawa et al. [40], Nguyen et al. [25], and Tayal and Khan [51]. We modeled the scission process with a set of 'master equations', or simple rate equations which, when rewritten in matrix form, transform the initial, experimentally obtained molar mass distribution data through a cascade of steps that mimic the multiple passes through the capillary system. With reasonable physical assumptions and a small number of physically motivated, adjustable parameters, this model is able to reproduce the successive molar mass distributions found experimentally, such as those shown in Fig. 3(a)–(c). Furthermore, the resultant model parameters yield fundamental, quantitative information about the scission process and why modifications to the experimental conditions (pressure, relative concentration (c/c^*), etc.) lead to different results.

The model relies on two basic assumptions. First, we assume that, consistent with prior experimental observations, stretched polymer chains tend to break predominantly around their mid-point, where the tension due to (transient) elongational forces reaches its maximum value [15]. Second, the model assumes that longer polymer chains have a higher probability of breaking in a given interval of time Δt, again consistent with previous observations by other groups [40]. Unlike previous models, however, we treat these two assumptions separately and adopt flexible fitting functions that allow for both assumptions to be violated. We make no other a priori assumptions about the breakage of the molecules and as we shall see, both the existence of a minimum molecular size for scission and the tendency for a chain to break near its middle point will emerge naturally from our modeling of the experimental data.

Let $n_i(t)$ be the number fraction of molecules of size i at time t, and $A_{i \leftarrow j} \equiv A_{ij}$ be the probability for a molecule of size j to be broken into pieces of size i and $j - i$ (with $j > i$, where i and j are integers such that $i, j \in [1 \ldots N_{max}]$) during a given interval of time Δt. We thus start by discretizing the initial experimental molar mass distribution $n_i(0)$ into $N_{max} = 200$ different molecular sizes. Note that the actual value of N_{max} does not affect the results of the calculations (all sufficiently large values of N_{max} lead to the same extent of agreement with experimental data); however, choosing a relatively small value of N_{max} greatly expedites the numerical calculations. One can then write a set of rate equations for the evolution of the populations $n_i(t)$ as a

function of time. A typical rate equation for a single molecular mass i simply reads

$$n_i(t+\Delta t) - n_i(t) = -n_i(t)\sum_{j=1}^{i-1} A_{ji} + \sum_{j=i+1}^{N_{\max}} n_j(t)A_{ij} \tag{3}$$

The left-hand side of the equation gives the change in the population of molecules of size i during the period of time Δt. The first term on the right-hand side represents the scission of molecules of size i into two smaller molecules (of sizes j and $i-j$, with $j<i$), while the second term represents the formation of molecules of size i as the by-product of the scission of larger molecules (of size $j>i$). This set of linear equations can be written in matrix form as

$$n(t+\Delta t) - n(t) = An(t) \tag{4}$$

where $n(t) = \{n_1(t), n_2(t), \ldots n_{Nmax}(t)\}$ is the column vector that describes the number fraction molar mass distribution and $A = A(t, \Delta t)$ is a transition matrix that contains information about the most probable statistics of the chain breakage process during the period of time Δt at time t. Note that this equation can also be written as $n(t+\Delta t) = (A+I)n(t)$, where I is the $N_{\max} \times N_{\max}$ identity matrix; this form is often more practical from a computational point of view. The global matrix $A+I$ thus transforms the molecular size distribution $n(t)$ to $n(t+\Delta t)$.

In the $\Delta t \to 0$ limit, one can rewrite Eq. (3) as a set of differential equations, which is the standard way to deal with such problems when the shear is constant in time and uniform in space [40,51]. Indeed, if A is constant, one can in fact solve these equations exactly, as illustrated by Ballauff and Wolf [16,39]. However, we have a transient elongational flow in our case because the chain must go through the converging stream lines at the entrance of the narrow capillary [18]. Therefore, it is not possible to write a continuous time description of the process because it would require a precise knowledge of the time- and position-dependent matrix A. An alternative would be to carry out detailed computer simulations (e.g. using a molecular dynamics algorithm) of the dynamics of polymer chains in the converging flow [18]. Such simulations can provide useful information about the microscopic phenomena involved in the scission of individual chains, but cannot easily be used to analyze experimental data. Instead, we treat each pass as a sequence of $q \geq 1$ periods of time of duration Δt, and we use q as a fitting variable. We further assume that there exists an effective matrix A which reproduces the average effect of the shear during these periods of time Δt. In other words, we replace the (unknown) matrices $\{A(t=\Delta t), A(t=2\Delta t), \ldots, A(t=q\Delta t)\}$ that would be needed to properly calculate the scission statistics of the chains as they move through the high-shear region in a total period of time $q\Delta t$, by a single effective matrix A. Note that the actual matrix elements of A will be a function of q since in effect we are carrying out the following substitution:

$$\prod_{i=1}^{q} (A(i\Delta t) + I) \to (A+I)^q \tag{5}$$

As far as we can tell, this represents the first modeling of transient elongational flow degradation by effective kinetic equations and transformation matrices. This approach, together with the matrix elements described below, gives us full control over the parameters of the model and makes it easier to draw conclusions from their values, as we shall see. Note that these equations are conservative, in the sense that the total molar mass is a conserved quantity. It is also important to keep in mind that because the molar mass distribution and the viscosity of the solution change after each pass, the effective matrix A may in principle evolve from pass to pass.

An important part of our model is the choice of matrix elements A_{ij}. The latter are written as

$$A_{ij} = \begin{cases} 2S(i,j)P(j) & \text{for } i<j \\ -P(j) & \text{for } i=j \\ 0 & \text{for } i>j \end{cases} \tag{6}$$

where $P(j) = \sum_{i=1}^{j-1} A_{ij}$ denotes the total probability of breaking a molecule of length j during the period Δt, and $S(i \leftarrow j) \equiv S(i,j)$ is the probability that such an event generates molecules of size i and $j-i$. The factor of two arises from the fact that the function $S(i,j)$ is assumed to be symmetric about the center of the molecule ($j = i/2$) : the term $S(i,j)P(j) + S(i,i-j)P(j)$ then reduces to $2S(i,j)P(j)$. The terms $A_{ii} = -P(i)$ along the main diagonal give the total probability for a molecule of size j to be broken during that period of time, while the lower diagonal elements are null. These elements are null for the reason that we have not allowed, in this version of the model, chain recombination of fragments to form larger molecules. This choice of matrix elements explicitly decouples the probability of scission per unit time, $P(j)$, and the location of the scission along the chain $S(i,j)$.

The total probability of breakage $P(j)$ is a key parameter of all scission models. Instead of choosing an ad hoc function, which is generally the case with kinetic models, we propose the simple and very flexible step-like cutoff function

$$P(j) = \tanh\left[\left(\frac{j}{m_0}\right)^{\alpha}\right] \tag{7}$$

for the total probability of scission during the period of time Δt. Therefore, m_0 is roughly the molar mass cutoff for the scission while the exponent α is a measure of the effective sharpness of the cutoff. In fact, $P(j)$ becomes a sharp, step-like Heaviside function $H(m_0)$ when $\alpha \to \infty$ and a flat function, $P(j) = 1$, in the $\alpha \to 0$ limit. Moreover, the selected $P(j)$ function increases linearly with size j if $\alpha = 1$ and m_0 is larger than the largest molecular size ($N_{\max}$) in

the system. This function can thus represent a wide range of behaviors, from sharp molecular thresholds for scission to size-independent scission probabilities. This approach is both more flexible and more general than previous ones in the literature [40]. In its current version, the model does not have an explicit probability for the molecules not to be affected by the elongational flow field during the period of time Δt; this is equivalent to assuming that all the molecules (on average) feel a similar effective elongational flow field at the entrance of the capillary. The strain rate distribution is difficult to project onto the model, given that the flow within the capillary tube exceeded the turbulent boundary, thereby rendering the flow unsteady. Although this is not an accurate description of the transient elongational flow present here, one should keep in mind that the matrix A represents an average description of the breaking process over a macroscopic time Δt here because we do not use a continuous time approach. In fact, we did study the problem with the function $P(j) = P_\infty tanh[(j/m_0)^\alpha]$, where the prefactor P_∞ was used to control the probability of not breaking during the given time period, but the results led to essentially the same quantitative agreement as those reported here (not shown). Therefore, this assumption ($P_\infty = 1$) does not appear to affect the ability of the model to describe the statistical properties of the polymer solutions after each pass.

We model the distribution $S(i,j)$ of breaks along the chain by a normalized truncated Gaussian distribution centered around the middle point of the chain (monomer $j/2$) and with a standard deviation σ :

$$S(i,j) = C^* \exp\left[-\frac{(i - j/2)^2}{2\sigma(j)^2} \right] \tag{8}$$

where C^* is a normalization constant defined by

$$\frac{1}{C^*} = \sum_{i=1}^{j-1} \exp\left[-\frac{(i - j/2)^2}{2\sigma(j)^2} \right] \tag{9}$$

We further use $\sigma = \sigma(j) = j \times \sigma_0$, i.e. the width of the distribution increases linearly with the molecular size j of the molecule that is being broken into two pieces. The parameter σ_0 can be thought of as a percentage of the total chain length that is susceptible to chain breakage. Hence, $\sigma_0 \to 0$ implies purely midpoint scission ($i = j/2$), while larger values of σ_0 create an increasingly random distribution of scission points along the chain (for instance, $j_0 \gg 1$ would correspond to a uniform probability of breaking the chain at any position). Again, our choice of modeling function allows essentially all possible types of behaviors to be recovered (for example random, central, or Gaussian scission). In this way, data analysis can give us fundamental information about the scission process with minimal ad hoc hypotheses.

The problem is thus reduced to finding the combination of parameters $\{\alpha, m_0, \sigma_0, q\}$ that reproduces the experimental observations. Note that because we decoupled the probability functions $P(j)$ and $S(i,j)$, and because of our specific choice of functions and free parameters, we do not need to choose a particular model for the scission, unlike some of the previous studies [16,51]. Instead, the values found for the fitting parameters will provide this information in a natural way, and the type of scission emerges naturally from the model.

In the unit system that we have defined, the residence time of the molecules in the high-strain region of the extensional flow field is $q\Delta t$. Since the total probability of breaking a molecule is $P(j)$ during each period of time Δt, Δt is directly related to the mean lifetime of an intact long molecule (for which $P(j) = 1$) in the high-strain region. As we will see, our analysis will find $q > 1$, which means that on average, each long molecule is involved in a cascade of $q > 1$ consecutive breaking processes during a given pass through the elongational flow field. In other words, according to this modeling of our experimental data, the mean residence time in the high-strain region is at least twice as large as the mean lifetime of the larger molecules in this strain field. Mathematically, this means that in order to reproduce the distribution function after each pass, we need to iterate the application of Eq. (4) to the molar mass data at least two times (in particular, it is impossible to explain the data after the first pass, even approximately, if we assume that $q = 1$). A complete study of the lifetimes and residence times will be presented elsewhere.

To be conservative we chose $q = 2$ and, in order to model the behavior of the differential weight fraction distributions, the three remaining parameters $\{\alpha, m_0, \sigma_0\}$ are those which minimize an error function which is based on the weighted differences between the calculated mean (or peak position), variance (or PDI), and skew (or peak asymmetry) of the model distribution and those values from the experimental data. The quality of the calculated distributions is gauged using the following function, which describes a relative error of the fit to the data in terms of the mean, μ, variance, σ, and skew γ. This function is the weighted sum of the relative errors in the properties of the calculated distributions relative to the experimental distributions, i.e.

$$f_{\text{error}} = A1\left(\left|\frac{\sigma_e - \sigma_c}{\sigma_e}\right|\right) + A2\left(\left|\frac{\mu_e - \mu_c}{\mu_e}\right|\right) + A3\left(\left|\frac{\gamma_e - \gamma_c}{\gamma_e}\right|\right) \tag{10}$$

the subscripts e and c refer to experimental and calculated values respectively. The parameters $A1$, $A2$ and $A3$ are constants which control the weight of each error on the fit. Values of $A1 = 2.5$, $A2 = 1$, and $A3 = 1$ were found to be optimal for reproducing the experimental data. Alternatively one can also use a least squares fit by comparing the calculated distributions and the experimental distributions at each step [16,39]. However, we decided that given the noise in the data, our approach is preferable because it

focuses on general trends in the distribution and not on the local details of the data.

In order to obtain the optimal values of these parameters we carried out a simple grid search of the $\{\alpha, m_0, \sigma_0\}$ parameter space to obtain the values that minimize this error function. Remarkably, we found that in almost all cases, $\sigma_0 \in [0.09, 1.15]$ was optimal for reproducing the experimental distributions. To further simplify, we thus fixed σ_0 with the average value for each data set and we minimized the fitness function for the other two parameters (these values are listed later). Note that previous modeling studies have often arbitrarily taken a value of $\sigma_0 = 0.2$ [40,51]. Yet our data analysis shows that in the transient extensional flow field we created, the distribution of chain breakage points is, in fact, more tightly centered around the middle of the chain. Moreover, the value of σ_0 emerges naturally from our minimization procedure.

To illustrate the agreement between the model and the experimental data, Fig. 4(a) shows a typical data set and our calculated distributions corresponding to data for an LPA experiment such as that shown in Fig. 3(a). The agreement is generally very good, though the calculated distributions sometimes slightly underestimate the peak height. A key point is that in order to achieve good quantitative agreement, we require at least $q = 2$. As mentioned above, this is especially the case when reproducing the first-pass distribution data, which makes sense since the initial distribution has a large number of very long chains. Fig. 4(b) and (c) shows the calculated and experimental distributions for the DMA and PEO samples, respectively.

In order to illustrate the behavior of the model parameters, Table 1 shows some typical results for $\{\alpha, m_0\}$, when σ_0 is chosen to be equal to 0.12. Interestingly, we see that the exponent α is a monotonically increasing function of the experimental pass number, which implies that $P(j)$ converges toward a step-like function. The initial α value of unity is fully consistent with previous assumptions of linear increases in $P(j)$ [40,51], but latter passes produce step-like functions that were not predicted by previous approaches. On the other hand, the critical size m_0 is a decreasing function of the number of passes (excluding the first pass). We are presently investigating the reasons for this pass-to-pass variation in m_0. It has been shown that a polymer solution (in a flow field) which is well below its entanglement threshold most likely will not be modified by the addition of polymer molecules [52]. Although it was determined for LPA that the 0.1% (w/v) (zero-pass) polymer solution was above the entanglement threshold c^*, in each subsequent pass the polymer solution was somewhat below c^*. Therefore, it is possible that the first-pass results are affected by interchain entanglements, as previously mentioned, and this could explain the smaller value of m_0 we found. The presence of entanglements might, for example, affect the critical molar mass value below which the molecules do not undergo scission [43–46]. One related, possible explanation of the later pass-to-pass reduction in m_0 is that, at constant pressure, a decrease in average molar mass leads to an increase of velocity and strain, hence a decrease of the minimum molecular size that can be broken in the device. In any case, these two trends (decrease of the critical molecular size m_0 and increase of the exponent α) indicate that the chain scission process at the capillary entrance naturally generates narrow molar mass distributions of 'small' polymers that cannot be broken any further in the given (fixed) strain (estimated for these experiments by the method of Metzner and Metzner to be about 45,000 s^{-1}) [21]. This is critical for the purpose of generating monodisperse polymer solutions.

Table 1
Table of calculated model parameters $\{\alpha, m_0\}$ for $\sigma_0 = 0.12$. These data correspond to the calculated distributions of LPA molar mass shown in Fig. 4(a)

Pass number	α	m_0 ($\times 10^{-3}$ g/mol)
1	1	2000
2	3	3100
3	6	1700
4	9	1600
5	10	1200

Finally, we can predict how the molar mass distribution would evolve with further passes if we assume that the parameters $\{\alpha, m_0\}$ do not vary anymore after pass five. Fig. 4(a) also contains the extrapolated distribution for 50 passes under the assumption that the parameters $\{\alpha, m_0\}$ have already reached their asymptotic values, $\alpha = 10$ and $m_0 = 1200 \times 10^3$ g/mol. Here, we predict a $M_w = 546 \times 10^3$ g/mol and a PDI = 1.077.

4. Conclusions

This study has demonstrated for the first time the potential of high-velocity capillary entrance flow to provide a general route to the creation of low-polydispersity high polymers, through a systematic reduction in PDI and M_w obtained by multiple passes through a well-defined contraction. It has never been shown before that such low PDI values (1.12–1.15) could be obtained via chain degradation, particularly for such high molar mass polymers (>200,000 g/mol). Experiments with the three different polymers yielded qualitatively similar molar mass distribution shifts and PDI decreases. While the finding is in this sense remarkable, an examination of the literature provides many clues which makes it surprising that this was not discovered long ago.

The method of elongational polymer degradation and polydispersity reduction that we describe here appears to be purely physical in nature. We have repeated these experiments many times and, in all cases, we noted the final PDI after five passes through the capillary to be in the range of 1.12–1.17 when capillaries with ID $\geq$ 150 μm

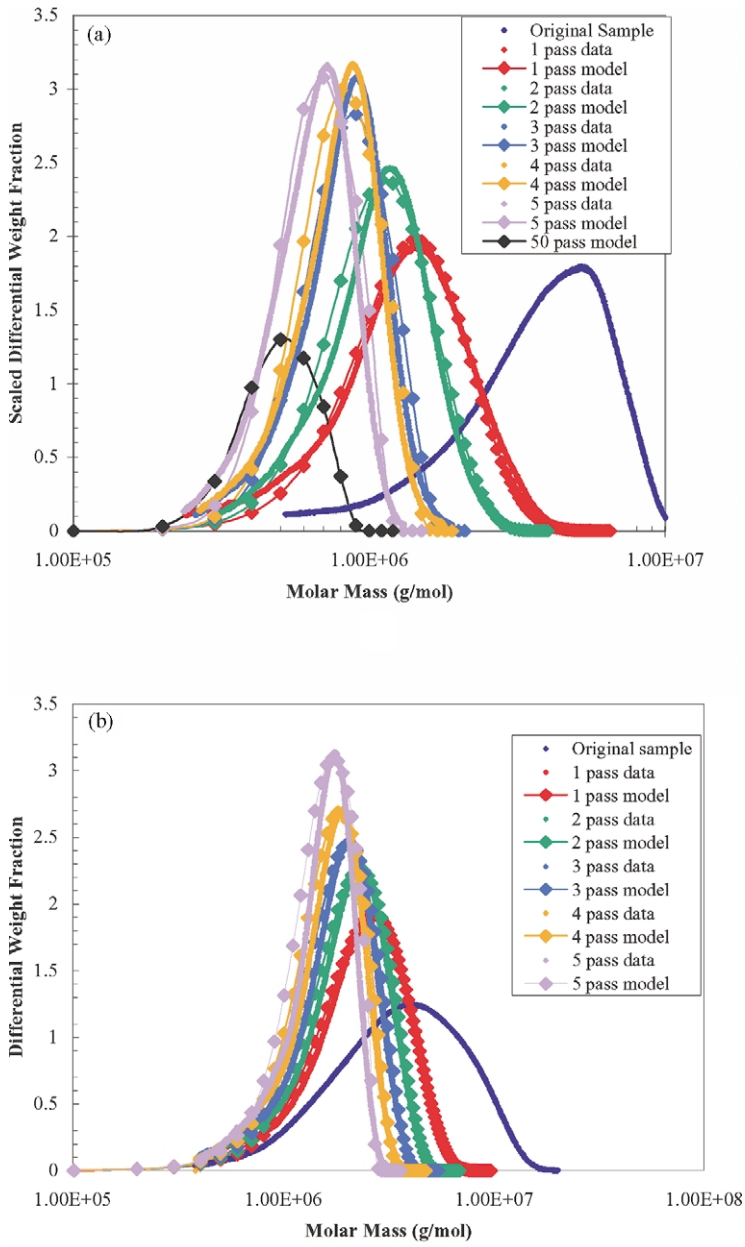

Fig. 4. Calculated and experimental molar mass distributions for (a) linear polyacrylamide, (b) polydimethylacrylamide, and (c) poly(ethylene oxide) solutions passed through the capillary entrances. Calculated distributions are shown with data points. The symbols correspond to the calculated distributions and the solid curves correspond to the experimental distributions. The distributions are generated from the normalized number fraction distributions; as a result their peak heights differ from the original molar mass distributions by a constant value. Experimental conditions are given in the Fig. 3 caption.

were used. We always observed most of the degradation to occur during the first pass, with the amount of degradation decreasing as the average molar mass shifted towards the critical molecular size m_0.

The results of our experiments in the application of a specific transient elongational flow field to high polymers suggest a novel method for the generation of diverse classes of monodisperse polymers of a relatively high molar mass. While so far we have only applied it to water-soluble polymers, the method appears to have good potential for broad applicability. The iterative nature of the method provides an additional degree of control over the final product. Elongational flow fields created by capillary contractions could be placed 'in parallel,' with polymer solutions automatically cycled through multiple passes under pressure to allow higher-throughput polymer processing, potentially producing monodisperse high polymers in quantities which are not feasible for production by any method save specialized chemical synthesis. (Note that in our experiments, the polymer mass flow rate through a

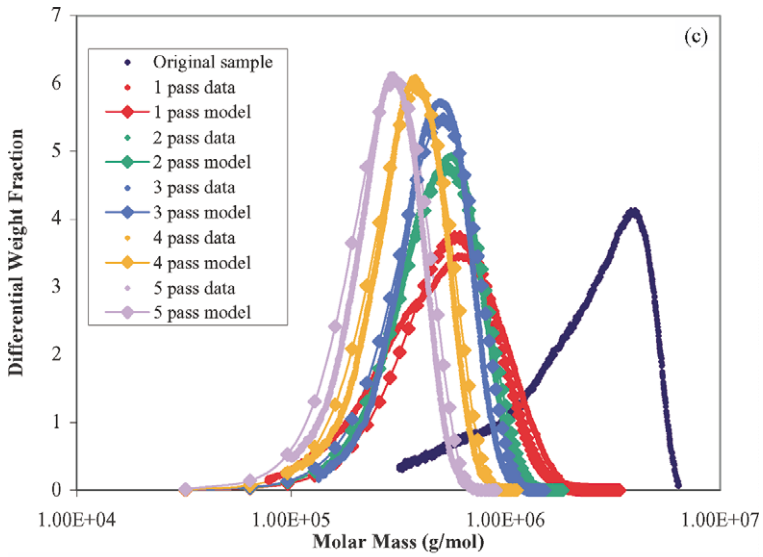

Fig. 4 (*continued*)

single capillary was 1 mg/s; hence with 1000 capillaries in parallel one could process 1 g/s). This method could provide a simple means to obtain monodisperse samples of some classes of polymers that are not conveniently synthesized by chemical methods, and hence are not easily accessed at high molar mass with low PDI, by any other means except preparative chromatography.

We developed a novel mathematical approach to model the experimental data, which explains the results and which has given us a better understanding of the characteristics of the chain scission process. The statistical model, which decouples the temporal (P) and spatial (S) probability functions and uses only three parameters to parameterize a wide range of possible functions, clearly indicates that as might be expected from previous work, the chains break multiple times at each pass ($q > 1$), and that the fixed strain rate cannot break molecules below a given molecular size ($\sim m_0$). Moreover, we find that the chains break over a much narrower region ($\sigma_0 = 0.12$) than previously assumed. It is these combined effects that allow us to generate increasingly monodisperse polymer solutions with only a few passes through the capillary entrance. A more detailed study of the relationship between the process parameters $\{\alpha, m_0, \sigma_0, q\}$ and the experimental conditions is currently in progress.

Acknowledgements

A.E.B. and B.A.B. acknowledge the Arnold and Mabel Beckman Foundation (Beckman Young Investigator Award) for support, and would like to thank Dr Wesley Burghardt and Victor Beck for helpful discussions on the subject and Donald H. Heckenberg for initial work on the project. G.W.S. and M.K. acknowledge a Research Grant and a Scholarship, respectively, from the Natural Sciences and Engineering Research Council of Canada (NSERC). M.K. would also like to thank the University of Ottawa for a National Excellence scholarship.

References

[1] Lee W, Lee H, Cha J, Chang T, Hanley KJ, Lodge TP. Macromolecules 2000;33:5111–5.
[2] Trzaska ST, Lee L-BW, Register RA. Macromolecules 2000;33:9215–21.
[3] Maughon BR, Morita T, Bielawski CW, Grubbs RH. Macromolecules 2000;33:1929–35.
[4] Hirao A, Nakahama S. Acta Polym 1998;49:133–44.
[5] Redakcji O, Qiu J, Charleux B, Matyjaszewski K. Polimery 2001;46:453–60.
[6] Matyjaszewski K. Macromol Symp 2001;174:51–67.
[7] Qiu J, Charleux B, Matyjaszewski K. Polimery 2001;46:663–72.
[8] Maynard HD, Okada SY, Grubbs RH. Macromolecules 2000;33:6239–48.
[9] Bielawski CW, Grubbs RH. Macromolecules 2001;34:8838–40.
[10] Kobayashi M, Okuyama S, Ishizone T, Nakahama S. Macromolecules 1999;32:6466–77.
[11] Staudinger H. Die Hochmolekularen Organischen Verbindugen. Berlin: Verlag Von Julius Springer; 1932.
[12] Kuhn W. Ber Chem Dtsch Ges 1930;63:1503–9.
[13] Kuhn WZ. Physik Chem (A) 1932;161:427–40.
[14] Montroll EW, Simha R. J Chem Phys 1940;8:721–7.
[15] Frenkel J. Acta Physicochim URSS 1944;19:51–76.
[16] Ballauff M, Wolf BA. Macromolecules 1981;14:654–8.
[17] Reese HR, Zimm BH. J Chem Phys 1990;92:2650–62.
[18] Knudsen KD, Cifre JGH, de la Torre JG. Macromolecules 1996;29:3603–10.
[19] Nguyen TQ, Kausch HH. Polymer 1992;33:2611–21.
[20] Odell JA, Keller A, Rabin Y. J Chem Phys 1988;88:4022–8.
[21] Metzner AB, Metzner AP. Rheol Acta 1970;9:174–81.
[22] Merrill EW, Leopairat P. Polym Engng Sci 1980;20:505–11.

[23] Nguyen TQ, Kausch HH. Chimia 1986;40:129–35.
[24] Nguyen TQ, Kausch HH. J Non-Newtonian Fluid Mech 1988;30: 125–40.
[25] Nguyen TQ, Liang QZ, Kausch HH. Polymer 1997;38:3783–93.
[26] Nguyen TQ. Chimia 2001;55:147–54.
[27] Quinzani LM, Armstrong RC, Brown RA. J Rheol 1995;39:1201–28.
[28] Quinzani LM, Armstrong RC, Brown RA. J Non-Newtonian Fluid Mech 1994;52:1–36.
[29] Boger DV, Crochet MJ, Keiller RA. J Non-Newtonian Fluid Mech 1992;44:267–79.
[30] Coates PJ, Armstrong RC, Brown RA. J Non-Newtonian Fluid Mech 1992;42:141–88.
[31] Odell JA, Keller A, Miles MJ. Polym Commun 1983;24:7–10.
[32] Keller A, Odell JA. Colloid Polym Sci 1985;263:181–201.
[33] Odell JA, Keller A. J Polym Sci: Part B: Polym Phys 1986;24: 1889–916.
[34] Muller AJ, Odell JA, Keller A. Polym Commun 1989;30:298–301.
[35] Narh KA, Odell JA, Muller AJ, Keller A. Polym Commun 1990;31: 2–6.
[36] Odell JA, Muller AJ, Narh KA, Keller A. Macromolecules 1990;23: 3092–103.
[37] Muller AJ, Odell JA, Carrington S. Polymer 1992;33:2598–604.
[38] Odell JA, Keller A, Muller AJ. Colloid Polym Sci 1992;270:307–24.
[39] Ballauff M, Wolf BA. Macromolecules 1984;17:209–16.
[40] Tanigawa M, Suzoto M, Fukudome K, Yamaoka K. Macromolecules 1996;29:7418–25.
[41] Buchholz BA. Electrophoresis 2001;22:4118–28.
[42] Larson RG. The Structure and Rheology of Complex Fluids. New York: Oxford University Press; 1999.
[43] Harrington RE, Zimm BH. J Phys Chem 1965;69:161–75.
[44] Bestul AB. J Chem Phys 1960;32:350–6.
[45] Glynn PAR, Van Der Hoff BME, Reilly PM. J Macromol Sci-Chem A6 1972;8:1653–64.
[46] Bueche F. J Appl Polym Sci 1960;4:101–6.
[47] Broseta D, Liebler L, Lapp A, Strazielle C. Europhys Lett 1986;2: 733–7.
[48] Bird RB, Armstrong RC, Hassager O. Dynamics of Polymeric Liquids. New York: Wiley; 1987.
[49] Horn AF, Merrill EW. Nature 1984;312:140–1.
[50] Jones DM, Walters K. Rheol Acta 1989;28:482–98.
[51] Tayal A, Khan SA. Macromolecules 2000;33:9488–93.
[52] Carrington SP, Tatham JP, Odell JA, Saez AE. Polymer 1997;38: 4151–64.